

# PLASMA ENHANCED CVD OF AMORPHOUS HYDROGENATED SILICON INVESTIGATED BY OPTICAL DIAGNOSTICS

D. Mataras and D.E. Rapakoulias  
*Department of Chemical Engineering*  
*University of Patras, GR 261 10 Patras, Greece*

## ABSTRACT

The usefulness of optical diagnostics for the investigation of gas discharges is outlined through the presentation of the application of Laser Induced Fluorescence, Spatially Resolved Optical Emission, and Laser Scattering, in PE-CVD of a-Si:H. Spatial profiles of SiH and SiH<sup>+</sup> radicals and particle scattered light are presented in various discharge conditions. Their information content is analyzed, and the possibility of correlation with discharge and film characteristics is presented.

## INTRODUCTION

Plasma Enhanced (or Plasma Assisted) CVD is today the standard manufacturing process for a large variety of materials with electrical properties ranging from insulators to semi- and superconductors. Among these materials, a-Si:H, and its alloys with various elements, like C, N, F, Cl, Ge, have been the subject of a very large number of studies in the last 15 years. The scientific interest for these materials comes from the large number of their potential applications, mainly for the fabrication of electronic devices. For example, a-Si:H is involved in the manufacturing process of six categories of commercially available devices, such as: solar cells, photoreceptors, photoconductors, thin film FET's, and high voltage thin film resistors, while other even more exciting applications are planned for the near future (1).

The study of PE-CVD of a-Si:H requires an interdisciplinary approach, like most of the processes used for manufacturing advanced materials. Therefore, a complete understanding of the process mechanisms would involve plasma chemistry and physics, fluid- and electro- dynamics, surface chemistry, and solid state physics. In

addition there are several, externally controlled, macroscopic parameters that have to be tuned appropriately to ensure the desired film quality. Thus, in the simplest case of the deposition of intrinsic a-Si:H from a pure rf silane discharge, one has to control at least the following parameters: gas pressure, flow rate, temperature of the deposition surface, level of rf power, and interelectrode distance. However, one can also list a series of additional process parameters which are not of minor importance, as for example: the base vacuum obtained and the bake-out time before the deposition, the level of impurities in the chamber and in the gases, the electrical characteristics of the chamber and the impedance matching network, and the rheologic characteristics of the chamber.

On the other hand, for an analytical approach of the issue there is need for a very large number of data concerning microscopic parameters, such as: number densities and energies of all species in the plasma (electrons, silane, radicals, positive and negative ions) as a function of space and time (during the rf cycle), collision cross sections, reaction rates, and sticking coefficients. Bearing in mind the fact that all these can be influenced by the macroscopic parameters, we can realize the degree of complexity of a self-consistent model describing the process.

Fortunately, the empirical or semi-empirical approach of tuning some parameters and examining the resulting film quality has worked out sufficiently well until now. This is why one can find a variety of operating conditions in the literature. Each research group has reached to a set of operating conditions, corresponding to their own deposition chamber, by a series of tuneup experiments which do not serve particularly for understanding the process.

Nevertheless, serious efforts have been concentrated in understanding the process, revealing the elementary process mechanisms and supplying data for a realistic simulation, by using several diagnostic techniques. Among these, optical and electrical diagnostics, which are commonly used for all glow discharge processes, have been a major source of significant information.

The first applications in silane plasma concerned the detection of the discharge light, by optical emission spectroscopy (OES), for the identification of electronically excited species and calculations of their rotational temperatures (2,3). But since these properties have given very little information about the process mechanism the research effort in this direction was soon discontinued. More sophisticated techniques like Spatially Resolved OES (4,5), Laser Induced Fluorescence (LIF) (4-9), Coherent Anti-Stokes Raman Spectroscopy (CARS) (10) and Infrared Laser Absorption Spectroscopy (IRLAS) (11-13) have been employed to give direct information (density, reaction rate, diffusivity) about ground state radicals which are the a-Si:H film precursors. The relative success of these experiments has stimulated new interpretations of their information content, and new applications in similar processes (14,15).

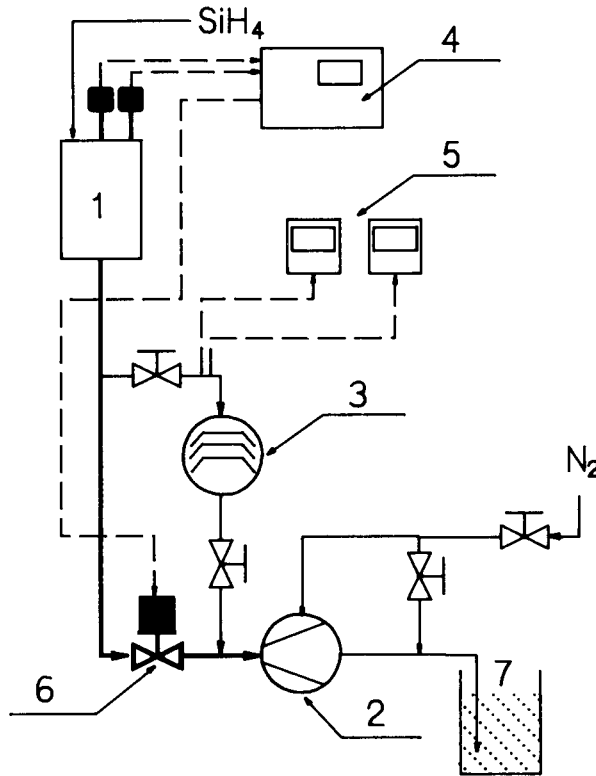


Figure 1. PE-CVD of a-Si:H experimental setup. (1) deposition chamber, (2) mechanical pump, (3) diffusion or turbo pump, (4) pressure control, (5) vacuum gages, (6) throttling valve, (7) KOH solution trap. Solid lines indicate the gas route, while, dotted lines are for measurement and control.

In the following paragraphs we will outline the possibilities to obtain useful information about the process, by presenting some of our results concerning the use of optical diagnostics in PE-CVD of a-Si:H from pure and diluted silane discharges.

## EXPERIMENTAL

A typical PE-CVD setup looks like the one presented in Fig.1. It consists mainly of a round stainless steel chamber equipped with viewports, and gas, electric and thermocouple feedthroughs. In this case the chamber diameter is 16 cm and the height is 20 cm and is very similar in construction with the much greater production chambers, although multichamber and rectangular apparatuses are also used. This simple construction is very suitable for experimental work and especially for the

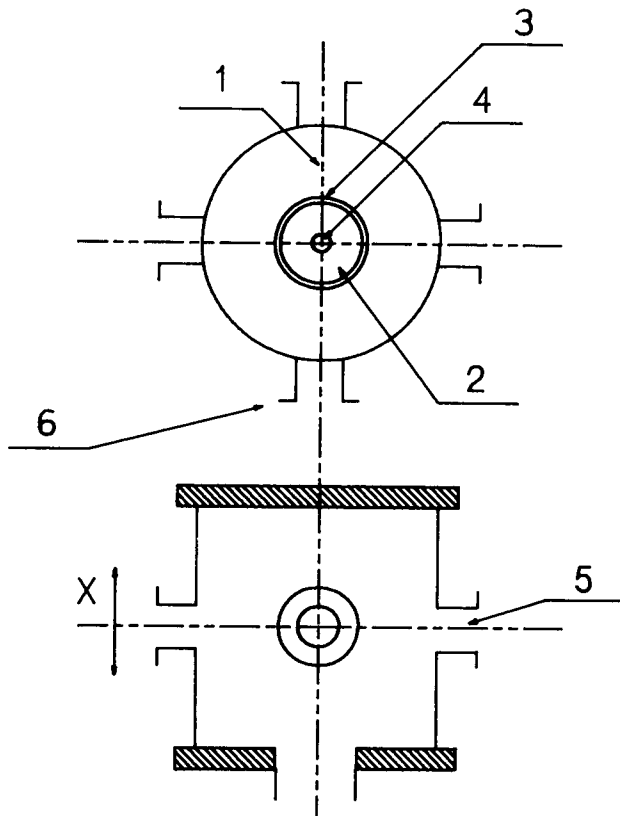


Figure 2. Deposition chamber for optical diagnostics. View from side (upper figure) and top (lower figure). (1) Laser beam path, (2) rf electrode, (3) rf shield, (4) flow splitter, (5) light collection path, (6) quartz viewports.

application of optical diagnostics. The experimental setup also includes vacuum pumps, gages, and equipment for accurate temperature, pressure, and flow control. Since silane is instantly flammable when exposed to air, some security measures are necessary. We are using nitrogen dilution of the effluent gas and a KOH solution trap.

In Fig.2 we present a schematic diagram of the deposition chamber used for LIF and OES diagnostics. The excitation source is a moderate-power Nitrogen-pumped dye-Laser. The fluorescence signal is collected at right angles with respect to the laser beam and focused through an interference filter to a PMT or a monochromator. The signal-to-noise ratio of the small voltage obtained from the PMT is intensified with a boxcar averaging technique. The emission signal from the same position of the chamber is collected by an optical fiber and focused to the entrance slit of a monochromator or a PMT.

Both the deposition process and the LIF-OES experiment can be completely automated with the use of microcomputers. The main difficulty in these experiments has to do with the need for a careful and precise alignment of the optical paths, and the signal acquisition procedure. Thus, in our effort to simplify the work of recording spatial intensity profiles, we have chosen to move the chamber instead of the optical path, and we have developed the much easier method of computer controlled acquisition by using only a fast digital storage oscilloscope instead of the boxcar (4).

## RESULTS AND DISCUSSION

LIF and OES have been used in a low pressure silane discharge to detect and record simultaneously the laser-excited fluorescence of SiH radicals and the spontaneous emission of electronically excited SiH<sup>\*</sup> radicals. Both species are produced through one-electron inelastic collisions with silane molecules, although their production mechanism is different. SiH represents one of the ground state radicals produced through the electron impact dissociation process, whereas SiH<sup>\*</sup> is a product of dissociative excitation. These two elementary processes differ mainly in their energetic requirements. Namely, emitting species have an appearance threshold of 10.4 eV, while dissociation products appear at about 8 eV. Consequently, there is a 2.5 eV difference in their appearance thresholds. Since these values are far above the mean electron energy (which is typically 2-3 eV), all the products of the decomposition of silane are formed by collisions with electrons that belong energetically to the tail of the electron energy distribution function (eedf). This eedf is characteristically bimodal because of the different electron production and acceleration mechanisms in different areas of the discharge, while the electron movement through the gas medium is anisotropic. Therefore, the production of these species will be sensitive to space and time variations. Moreover, one can expect that each one of these radicals will behave differently since their production depicts the relative behavior of different parts of the eedf.

Thus, intensity variations of these radicals as a function of space and as a function of various macroscopic parameters give information concerning the influence on their production processes and their specific power consumption.

In figures 3 and 4 we present characteristic LIF and OES axial profiles. Similar curves have been recorded for pressures between 15 and 100 mTorr in pure silane or up to 0.5 Torr for diluted silane. Additional experiments included the variation of power, flow-rate, gas composition, interelectrode distance, and electrode diameters (16).

These profiles represent the relative concentration of SiH and SiH<sup>\*</sup> radicals detected at each point of the interelectrode space. However, these measurements have to be regarded as the result of a mass balance between production and dissipation processes. The concentration of SiH radicals is strongly influenced by pressure, since they react fast with silane molecules (Fig.5). Thus, since diffusion of these species plays only a minor role for pressures above 20 mTorr, it is possible to

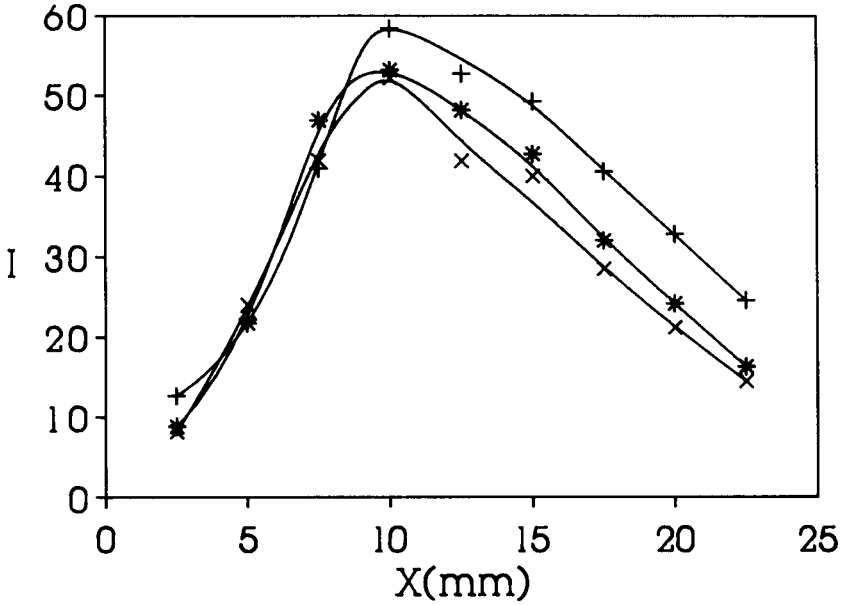


Figure 3. LIF Intensity ( $I$  in arbitrary units) as a function of sampled position ( $X$ ) in the interelectrode space, at three different pressures. (+) 21 mTorr, (\*) 39 mTorr, (x) 50 mTorr. ( $f=8$  sccm of pure silane,  $W=8$  Watts,  $d=25$  mm).  $X=0$  corresponds to the position of the rf electrode. Lines are drawn as a visual aid.

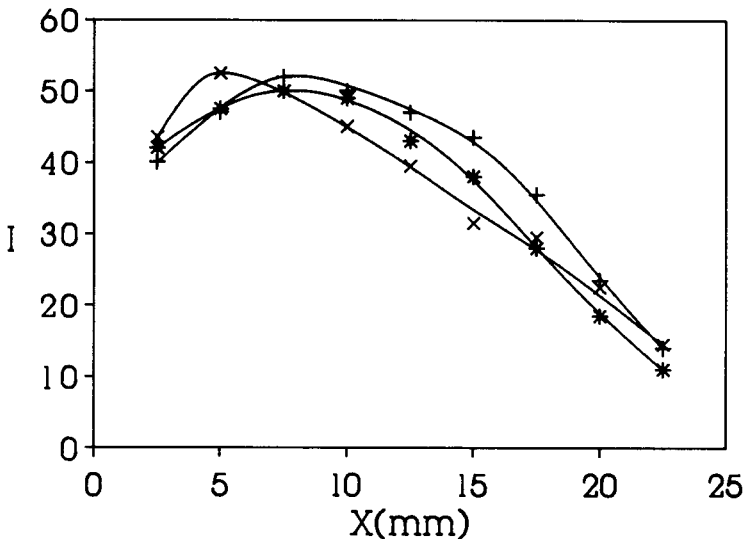


Figure 4. OES Intensity ( $I$  in arbitrary units) as a function of sampled position ( $X$ ) in the interelectrode space, at three different pressures. (+) 21 mTorr, (\*) 39 mTorr, (x) 50 mTorr. Same conditions as in Fig.3.

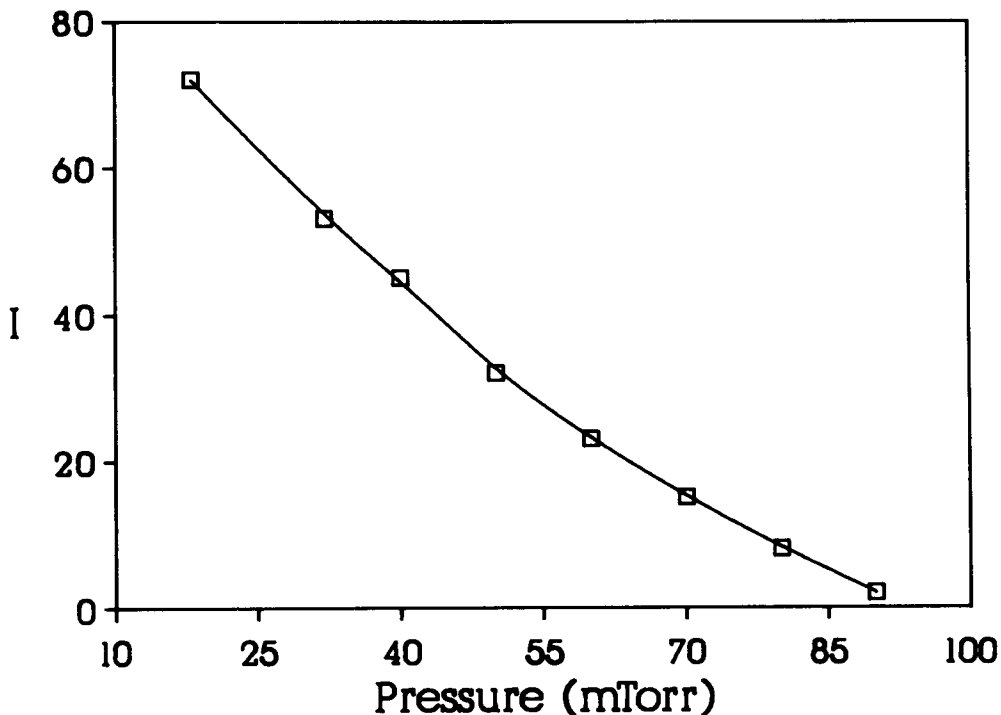


Figure 5. LIF intensity as a function of silane pressure. ( $f=11$  sccm,  $W=9$  Watts,  $d=25$  mm).

consider that LIF profiles represent the spatial generation profiles for all the other radicals in these conditions. In this case one can use normalized LIF profiles to calculate the concentration profiles of all the active radicals produced by the electron impact decomposition of silane, and consequently the flux of the radicals reaching the deposition surface (17). The actual concentration profiles of  $\text{SiH}_3$  radicals, which are believed to be the main film growth precursors, should be somewhat different from those of  $\text{SiH}$ , because diffusion plays a much more important role in this case. However, actual concentration profiles of  $\text{SiH}_3$  radicals measured by IRLAS are very similar to those of  $\text{SiH}$  presented here, in the sense that they also present a maximum around 8-10 mm, although the spatial intensity distribution is more uniform (13).

This approach contains several advantages over the previously proposed idea of using emission profiles as the spatial generation profiles (18,19). As one can observe in figures 3 and 4 emission profiles are sensitive to pressure variations while LIF profiles are not. Namely, the position of the LIF intensity maximum remains at the same distance from the rf electrode, while the position of the OES intensity maximum moves towards the rf electrode as pressure rises. The same behavior can be observed in the case of dilution with inert gases at exactly the same silane partial

pressure ( $P_{\text{SiH}_4}$ ). Additionally, when the pressure rises above 100-150 mTorr (depending on the power level), OES profiles present two intensity maxima located near each electrode. The first transition (occurring at 30-50 mTorr  $P_{\text{SiH}_4}$ ) is caused by the restriction of electron diffusion, while the second is caused by the  $\alpha$ - $\gamma$  transition (20).

These observations, along with additional data coming from the variation of discharge geometry, have lead to the conclusion that SiH radicals are produced by thermalized bulk electrons, while SiH<sup>\*</sup> radicals are produced by sheath-accelerated electrons. This is because the SiH<sup>\*</sup> concentration shows a strong dependence on the sheath magnitude and potential, whereas SiH is influenced more by the electron density in the bulk plasma.

The information obtained by these experiments justifies the hypothesis of a common radical generation profile and gives a series of data including new, interesting phenomena. For example the influence of interelectrode distance on radical generation has been correlated with a change in the film production rate (21), and the film quality, while the same methods have revealed an enhanced  $\gamma$  electron contribution in the case of silane dilution (22).

However, this is not the only useful information obtained by using optical diagnostics. The main problem in recording LIF is to avoid the generation of dust particles produced by homogeneous nucleation in the gas phase. This is also one of the major problems affecting the quality of the deposited films. This can be clearly observed in the SEM pictures of a-Si:H films deposited under conditions that favor the formation of particles (figures 6 and 7). As one can observe, these particles have a regular rhomboidal geometry indicating nucleation around charged particles.

Dust particles are believed to appear in relatively high power and/or pressures. However, our experiments have shown that this phenomenon occurs under some circumstances even at very low power and pressures as low as 20 mTorr. Thus, Laser scattering is a very sensitive method for studying this effect (23).

The creation of particles can be observed during the LIF experiments by a large increase of the time amplitude and the intensity of the laser signal. A characteristic light scattering profile is presented in Fig.8. This type of spatial profiles is observed in relatively high pressures. Particles begin to appear after several minutes of steady discharge operation and the evolution of their concentration is rather slow.

We have also observed another type of particle formation at low power and large interelectrode distance. In this case, the particles are mainly created near the center of the discharge, and they appear instantaneously. In the first case particles, are probably produced by a radical polymerization mechanism in high field regions of the discharge, while, in the second case, they are probably produced by ionic nucleation in low field regions (24).

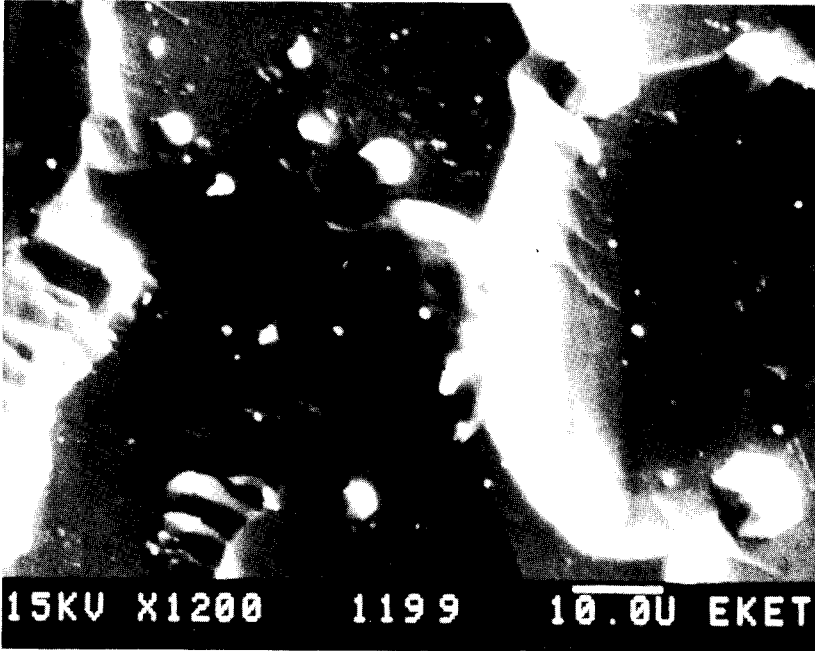


Figure 6. SEM picture of a-Si:H surface deposited on unpolished crystalline Si. Rhomboidal particles in SiH<sub>4</sub>-He mixture

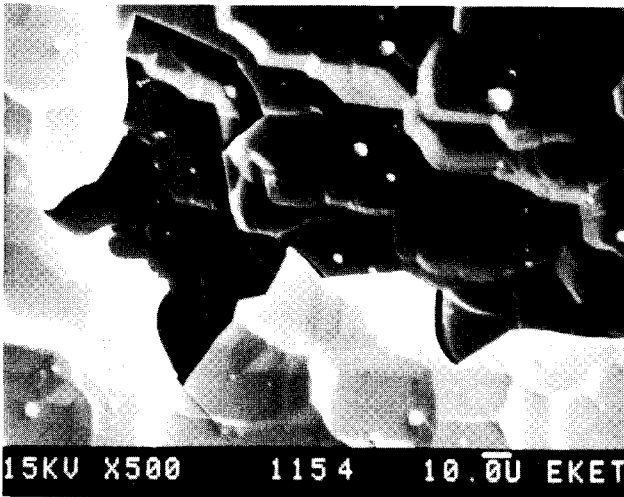


Figure 7. SEM picture of a-Si:H surface deposited on unpolished crystalline Si. Rhomboidal particles in SiH<sub>4</sub>-Ar mixture near a high stress surface crack.

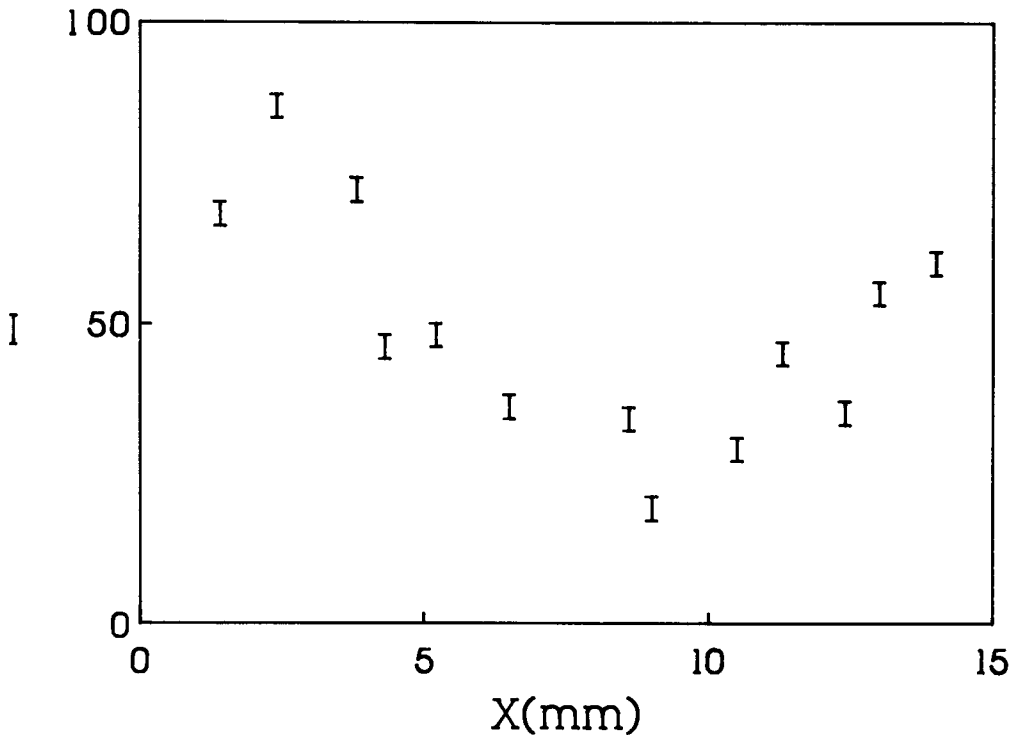


Figure 8. Scattered light intensity as a function of the sampled position in the interelectrode space. ( $P=350$  mTorr,  $f_{\text{SiH}_4}=6$  sccm,  $f_{\text{Ar}}=18$  sccm,  $W=40$  Watts,  $d=15$  mm)

### SUMMARY

Optical diagnostics are very suitable for the study of low pressure gas discharges. They can give meaningful, spatially resolved information about ground state, excited, and electrically charged species.

In the case of silane discharges, which are commonly used for the deposition of a-Si:H, they can give information about radicals that participate directly in the film growth. Also, one can obtain data concerning their production processes and the way they are influenced by the variation of macroscopic parameters. These observations can be correlated with the discharge and the film characteristics. Additionally, the collection of laser light scattered by dust particles can be used to obtain information about their generation processes.

In our case, the detection of SiH and SiH<sup>\*</sup> has revealed the fundamental differences in their production mechanism and has led to a better understanding of the process through the study of the influence of several macroscopic parameters.

### ACKNOWLEDGEMENTS

We wish to thank Mrs. B. Georgali of the Hellenic Cement Research Center for the SEM pictures. This work is supported by the "Non-Nuclear Energies" R&D program of the Commission of European Communities, DG XII

### REFERENCES

1. LeComber, P.G., in Winter European Course on Amorphous Silicon: The material and its optoelectronic applications, Folgaria-Italy, Task R&S S.r.l, (1989).
2. Perrin, J., and E. Delafosse, Journal of Physics D, Vol.13, p.759, (1980).
3. Kampas, F.J., and R.W. Griffith, Journal of Applied Physics, Vol.52, p.1285, (1981).
4. Mataras, D., S. Cavadias, D. Rapakoulias, Journal of Applied Physics, Vol.66, p.119, (1989).
5. Mataras, D., S. Cavadias, D. Rapakoulias, Proceedings of the "9th International Symposium on Plasma Chemistry", Pugnochiuso, Italy, September 1989, R. D'Agostino, ed., IUPAC, p.423,1293, (1989).
6. Schmitt, J.P.M, P. Gressier, M. Krishnan, G. De Rosny, J. Perrin, Chemical Physics, Vol.84, p.281, (1984).
7. Roth, R.M., K.G. Spears, G. Wong, Applied Physics Letters, Vol.45, p.28, (1984); Materials Research Society Symposium Proceedings, Vol.38, p.117, (1985).
8. Takubo, Y., Y. Takasugi, and M. Yamamoto, Journal of Applied Physics, Vol.64, p.1050, (1988).
9. Matsumi, Y., T. Hayashi, H. Yoshikawa, and S. Komiya, Journal of Vacuum Science and Technology A, Vol.4, p.1768, (1986).
10. Hata, N., A. Matsuda, and K. Tanaka, Journal of Non-Crystalline Solids, Vol.59-60, p.667, (1983).
11. Itabashi, N., K. Kato, N. Nishiwaki, T. Goto, C. Yamada, E. Hirota, Japanese Journal of Applied Physics, Vol.27, p.L1565, (1989).
12. Itabashi, N., K. Kato, N. Nishiwaki, T. Goto, C. Yamada, E. Hirota, Japanese Journal of Applied Physics, Vol.28, p.L325, (1989).

13. Itabashi, N., N. Nishiwaki, M. Magane, S. Naito, T. Goto, A. Matsuda, C. Yamada, and E. Hirota, *Japanese Journal of Applied Physics*, Vol.29, p.L505, (1990).
14. Tachibana, K., T. Mukai, A. Yuuki, Y. Matsui, H. Harima, *Japanese Journal of Applied Physics*, Vol.29, p.2156, (1990).
15. Tochikubo, F., A. Suzuki, S. Kakuta, Y. Terazono, T. Makabe, *Journal of Applied Physics*, Vol.68, p.5532, (1990).
16. Mataras, D., S. Cavadias, D. Rapakoulias, Submitted for publication to the *Journal of Applied Physics*.
17. Mataras, D., S. Cavadias, D. Rapakoulias, *Materials Research Society Symposium Proceedings*, Vol.169, (1989).
18. Gallagher, A., *Journal of Applied Physics*, Vol.63, p.2406, (1988).
19. Doughty, D.A., A. Gallagher, *Journal of Applied Physics*, Vol.67, p.139, (1990).
20. Perrin, J., P. Roca i Cabarrocas, and B. Allain, *Japanese Journal of Applied Physics*, Vol.27, p.2041, (1988).
21. Kounavis, P., E. Mytilineou, and D. Mataras, S. Cavadias, D. Rapakoulias, *Proceedings of the 20th International Conference on the Physics of Semiconductors*, Thessaloniki, Greece, August 1990, E.M. Anastasakis, G.D. Joannopoulos, eds., Vol.III, p.2115, World Scientific, (1990).
22. Mataras D., In Preparation.
23. Spears, K.G., R.P. Kampf, T.J. Robinson, *Journal of Physical Chemistry*, Vol.92, p.5297, (1988).
24. Gallagher, A., *Solar Cells*, Vol.21, p.147, (1987).